Quick Hosting Capacity Evaluation Based on Distributed Dispatching for Smart Distribution Network Planning with Distributed Generation

Bing Sun, Ruipeng Jing, Leijiao Ge, Yuan Zeng, Shimeng Dong, and Luyang Hou

***Abstract*—The smart distribution network (SDN) is integrating increasing distributed generation (DG) and energy storage (ES). Hosting capacity evaluation is important for SDN planning with DG. DG and ES are usually invested by users or a third party, and they may form friendly microgrids (MGs) and operate independently. Traditional centralized dispatching method no longer suits for hosting capacity evaluation of SDN. A quick hosting capacity evaluation method based on distributed optimal dispatching is proposed. Firstly, a multi-objective DG hosting capacity evaluation model is established, and the hosting capacity for DG is determined by the optimal DG planning schemes. The steady-state security region method is applied to speed up the solving process of the DG hosting capacity evaluation model. Then, the optimal dispatching models are established for MG and SDN respectively to realize the operating simulation. Under the distributed dispatching strategy, the dual-side optimal operation of SDN-MGs can be realized by several iterations of power exchange requirement. Finally, an SDN with four MGs is conducted considering multiple flexible resources. It shows that the DG hosting capacity of SDN oversteps the sum of the maximum active power demand and the rated branch capacity. Besides, the annual DG electricity oversteps the maximum active power demand value.**

***Index Terms*—Smart distribution network (SDN), microgrid, hosting capacity, multi-objective optimization, distributed optimal dispatching, flexible resource.**

NOMENCLATURE

α_1	0-1 variable denoting microgrid (MG) is in the state of purchasing power
α_2	0-1 variable denoting MG is in the state of selling power
$\alpha_{j,i}^{\mathrm{I}}$	Coefficient of active power injection of node i considering the upper current limit of node j
$\alpha_{j,i}^{\mathrm{V,m}}$	Coefficient of active power injection of node i considering the lower voltage limit of node j
$\alpha_{j,i}^{\mathrm{V,M}}$	Coefficient of active power injection of node i considering the upper voltage limit of node j
β_1	0-1 variable denoting smart distribution network (SDN) is in the state of purchasing power
β_2	0-1 variable denoting SDN is in the state of selling power
$\beta_{j,i}^{\mathrm{I}}$	Coefficient of reactive power injection of node i considering the upper current limit of node j
$\beta_{j,i}^{\mathrm{V,m}}$	Coefficient of reactive power injection of node i considering the lower voltage limit of node j
$\beta_{j,i}^{\mathrm{V,M}}$	Coefficient of reactive power injection of node i considering the upper voltage limit of node j
$\gamma_{s,t}^{\mathrm{OLTC}}$	0-1 variable denoting on-load tap changer (OLTC) gear at time t
ε	Convergence residuals
$\eta_{\mathrm{ES1,cha}}$, $\eta_{\mathrm{ES1,dis}}$	Charging and discharging coefficients of distributed energy storage (ES)
η_2	Loss coefficient of centralized ES
λ_{C}	The maximum change times of capacitor bank (CB) during a dispatching period
Ω_{SSSR}	Steady-state security region (SSSR) of SDN
$\Delta P_i^{\mathrm{PV}'}$	Updated capacity of photovoltaic (PV) at node i considering distributed ES
ΔP_x	Installed capacity of distributed generation (DG) at node i in the initial scheme
$\Delta P_N^{i,\mathrm{m}}$	Installed capacity of PV at node i considering the lower voltage limit of node N
$\Delta P_N^{i,\mathrm{M}}$	Installed capacity of PV at node i considering the upper voltage limit of node N
ΔP_{I}^i	Installed capacity of PV at node i considering branch current
ΔP_{V}^i	Installed capacity of PV at node i considering

Manuscript received: September 24, 2022; revised: February 1, 2023; accepted: March 28, 2023. Date of CrossCheck: March 28, 2023. Date of online publication: June 1, 2023.

This research was supported in part by the State Grid Scientific and Technological Projects of China (No. SGTYHT/21-JS-223), in part by the National Natural Science Foundation of China (No. 52277118), in part by the Tianjin Science and Technology Planning Project (No. 22ZLGCGX00050), and in part by the 67th Postdoctoral Fund and Independent Innovation Fund of Tianjin University in 2021.

B. Sun, R. Jing, L. Ge (corresponding author), and Y. Zeng are with the School of Electrical and Information Engineering, Tianjin University, Tianjin 300072, China (e-mail: sunbing@tju.edu.cn; rpjing@tju.edu.cn; legendglj99@tju.edu.cn; zengyuan@tju.edu.cn).

S. Dong is with State Grid Corporation of China, Beijing, China (e-mail: 18722131151@163.com).

L. Hou is with the School of Computer Science (National Pilot Software Engineering School), Beijing University of Posts and Telecommunications, Beijing, China (e-mail: luyang.hou@bupt.edu.cn).

DOI: 10.35833/MPCE.2022.000604

	node voltage
ΔP_i^{PV}	Installed capacity of PV at node i considering node voltage and branch current
Δt	Simulation timestep, i.e., 1 hour
ΔU	Total system voltage deviation
$b_{i,t}$	0-1 variable denoting the used CB number at node i at time t
C_1	Equal annual investment and maintenance costs of PV and distributed ES
C_2	Interaction cost with higher voltage power grid
C_3	Grid loss cost
C_4	Compensation cost to demand response (DR) user
C_5	Operation cost of centralized ES
C_{ES1}	Operation cost of charging/discharging 1 kWh electricity of distributed ES
C_{ES2}	Operation cost of charging/discharging 1 kWh electricity of centralized ES
C_t	Cost of 1 kWh grid loss at time t
C_{total}	Sum of C_1, C_2, C_3, C_4, and C_5
$C_{t,\mathrm{buy}}$	Price of purchasing electricity at time t
$C_{t,\mathrm{sell}}$	Price of selling electricity at time t
$C_{t,\mathrm{DR}}$	Subsidy cost of load reduction at time t
$C_{\mathrm{un,PV}}$	Unit investment cost of PV
$C_{\mathrm{un,ES1}}$	Unit investment cost of distributed ES
d_1	The lower limit factor of transferable load
d_2	The upper limit factor of transferable load
D	Set of DR users
day	Index of day
E	Branch set of SDN
$\boldsymbol{E}^{\mathrm{ES1}}$	Installed capacity vector of distributed ES
E_{ES1}	Total installed capacity of distributed ES in distribution system
E_i^{ES1}	Installed capacity of distributed ES at node i
E_i^{ES2}	Installed capacity of centralized ES at node i
$E_{i,t}^{\mathrm{ES1}}$	Electric energy of distributed ES at node i at time t
$E_{i,t}^{\mathrm{ES2}}$	Electric energy of centralized ES at node i at time t
$E_{i,1}^{\mathrm{ES1}}$	Electric energy of distributed ES at node i at the initial time of a dispatching period
$E_{i,T}^{\mathrm{ES1}}$	Electric energy of distributed ES at node i at the end time of a dispatching period
$E_{i,1}^{\mathrm{ES2}}$	Electric energy of centralized ES at node i at the initial time of a dispatching period
$E_{i,T}^{\mathrm{ES2}}$	Electric energy of centralized ES at node i at the end time of a dispatching period
$E_{i,t}^{\mathrm{ES2,1}}$	Electric energy loss of centralized ES at node i at time t
$H(i)$	Set of nodes that connected with node i
$I_{ij,\max}$	The upper limit of branch current
$\tilde{I}_{ij,t}$	Square value of branch current at time t
k_1	Weight coefficient of economy
k_2	Weight coefficient of node voltage deviation
$k_{\mathrm{inv,ES1}}$	Equal annual value coefficient of distributed ES investment
$k_{\mathrm{inv,PV}}$	Equal annual value coefficient of PV investment
$k_{\max}$	Square value of the upper limit for OLTC gear
k_{mim}	Square value of the lower limit for OLTC gear
$k_{\mathrm{om,ES1}}$	Equal annual value coefficient of distributed ES maintenance
$k_{\mathrm{om,PV}}$	Equal annual value coefficient of PV maintenance
k_s	Square value of gear s subtracts $s-1$
$k_{\mathrm{soc,m1}}$	Lower limit of state of charge (SOC) for distributed ES
$k_{\mathrm{soc,M1}}$	The upper limit of SOC for distributed ES
$k_{\mathrm{soc,m2}}$	The lower limit of SOC for centralized ES
$k_{\mathrm{soc,M2}}$	The upper limit of SOC for centralized ES
k_t	The square value of OLTC gear at time t
$n_{i,t}^{\mathrm{C}}$	Number of CBs used at node i at time t
$n_{i,\max}^{\mathrm{C}}$	The upper limit for number of CBs used at node i
$n_{i,\min}^{\mathrm{C}}$	The lower limit for number of CBs used at node i
N	Total node number in SDN
N_{int}	Nodes connected with PV in SDN
P_i	Active power at node i
P_i^{m}	The lower limit of active power injection at node i
P_i^{M}	The upper limit of active power injection at node i
$P_{\max}^{\mathrm{cap}}$	The upper limit for total installed capacity of PV
$\boldsymbol{P}^{\mathrm{PV}}$	Installed capacity vector of PV
P^{PV}	Total installed capacity of PV in SDN
P_i^{PV}	Installed capacity of PV at node i
$P_{i,t}^{\mathrm{ES1,cha}}$, $P_{i,t}^{\mathrm{ES1,dis}}$	Charging and discharging power of distributed ES at node i at time t
$P_{i,\max}^{\mathrm{ES1}}$	The upper limit for active power of distributed ES
$P_{i,t}^{\mathrm{ES2}}$	Discharging power of centralized ES at node i at time t
$P_{i,t,\mathrm{buy}}^{\mathrm{line}}$	Power purchased by MG at node i at time t
$P_{i,t,\mathrm{sell}}^{\mathrm{line}}$	Power sold by MG at node i at time t
$P_{i,t,\mathrm{buy}}^{\mathrm{net}}$	Power purchased by SDN at time t
$P_{i,t,\mathrm{sell}}^{\mathrm{net}}$	Power sold by SDN at time t
$P_{t,\mathrm{buy}}^{\mathrm{tra}}$	Power purchased from the higher voltage power grid by SDN at time t
$P_{t,\mathrm{sell}}^{\mathrm{tra}}$	Power sold to the higher voltage power grid by SDN at time t
$P_{i,t}^{\mathrm{load}}$	Adjusted power demand at node i at time t
$P_{i,t}^{\mathrm{ORG}}$	Original power demand at node i at time t
$P_{i,t}^{\mathrm{PV}}$	Equivalent PV output at node i at time t considering distributed ES
$P_{i,t,\max}^{\mathrm{PV}}$	Predicted PV output at node i at time t

$P_{ji,t}$	Active power flow from node j to node i at time t
$P_{mi,t}^{\text{SOP}}$	Active power flow from node m to node i at time t by soft open point (SOP)
Q_i	Reactive power at node i
Q_i^{m}	The lower limit of reactive power injection at node i
Q_i^{M}	The upper limit of reactive power injection at node i
Q_i^{C}	Capacity of one CB at node i
$Q_{i,t}^{\text{C}}$	Reactive power output of CB at node i at time t
$Q_{i,t}^{\text{ES2}}$	Reactive power output of centralized ES at node i at time t
$Q_{i,\max}^{\text{ES2}}$	The upper limit for reactive power output of centralized ES at node i
$Q_{i,t}^{\text{load}}$	Reactive power demand at node i at time t
$Q_{i,t}^{\text{SVG}}$	Reactive power output of static var generator (SVG) at node i at time t
$Q_{i,\max}^{\text{SVG}}$	The upper limit for reactive power adjustment of SVG at node i
$Q_{ji,t}$	Reactive power from node j to node i at time t
$Q_{mi,t}^{\text{SOP}}$	Reactive power from node m to node i at time t by SOP
R	Equivalent resistance between MG and SDN
r_{ij}	Branch resistance between node i and node j
$S(i)$	Set of nodes connected with node i by SOP
S_i^{ES2}	Apparent capacity of centralized ES at node i
S_i^{SOP}	Apparent capacity of SOP
T	A simulation period
$u_{i,t}$	Voltage deviation at node i at time t
$U_{i,t}$	Voltage at node i at time t
$U_{i,\text{rated}}$	Rated value of voltage at node i
$\tilde{U}_{i,t}$	Square value of voltage at node i at time t
$U_{i,\min}$	The lower limit of voltage at node i
$U_{i,\max}$	The upper limit of voltage at node i
$\boldsymbol{x}_\beta$	Vector of node injection power
x_{ij}	Branch reactance between node j and node i

I. Introduction

CHINA is rapidly expanding its distributed photovoltaic (PV) infrastructure [1], [2]. The evaluation of the hosting capacity for distributed generation (DG) is significant to guide the smart distribution network (SDN) to develop renewable energy. DG is often combined with distributed energy storage (ES) to integrate the distribution network in the form of microgrid (MG). However, the MGs are often invested by third-party companies. For privacy, the MG equipment cannot be dispatched by the distribution system operator (DSO) directly. The observability and controllability of the SDN decrease significantly, which might present a risk to the safe and economic operation [3], [4]. In the future, there will be a lot of flexible resources integrated into the SDN, e.g., soft open point (SOP) and demand response (DR), and they are complexly coupled together. Under the above complex background, more and more scholars begin to pay attention to the research on the DG hosting capacity of SDN. The research results can guide the installed capacity of DG in a distribution network.

For a certain distribution network (network topology and load characteristics are known), the access subject can maximize the benefits in the energy interaction process in a long-time scale to the maximum extent, on the premise of meeting a series of constraints such as power balance, capacity constraints, and operation security and stability [5], [6]. Currently, the capacity of the access subject is recorded as the hosting capacity of SDN. In other words, the DG hosting capacity of an SDN is determined by the optimal installed capacity and location of DG. Various models with different characteristics have been designed and investigated by researchers to evaluate the DG hosting capacity. A hierarchical optimization planning model was established in [7]. Grid loss cost, line investment cost, electricity purchase cost, and carbon emission cost were considered when evaluating the PV hosting capacity. In [8], a robust optimization model was proposed for evaluating the PV hosting capacity with spatio-temporal correlation. A two-layer coordination optimization planning model for distributed ES was proposed in [9]. A hosting capacity evaluation model was proposed for integrated energy system planning with DG considering both the DG output uncertainties and carbon emission punishments [10]. However, in the above optimization planning models, only the economy or voltage quality has been considered as the objective function items, and the comprehensive consideration should be included in the modeling. The impacts from the coordination action of ES and curtailing peak DG output were also ignored.

Economy and voltage quality parameters are both the key indicators in terms of the hosting capacity evaluation. These parameters must be obtained through sequential operation simulation, which can be divided into centralized optimization method [11], [12] and distributed optimization method [13], [14]. It is true that the centralized optimization method is often used for current distribution network operation simulation. The premise of centralized dispatching is that all equipment is modeled in a whole model. However, the DGs integrated into the distribution network are often invested by third-party companies. Besides, the communication delays and single-point failure are restricting the development of centralized optimization method. As such, the centralized optimization method is not always suitable for the SDN with multiple MGs [15]. Moreover, the load demand for real-time dispatching cannot be satisfied with a high proportion of renewable energy integration [16], [17]. Therefore, the architecture of distribution energy management system has changed from centralized dispatching to distributed dispatching. In order to realize the coordination optimization of SDN-MGs, an equivalent model based on non-iterative solution was studied for the first time in [18]. In [19], a two-layer model was established and solved by analytical target cascading. To realize the dual-side optimal operation of SDN-MGs, a changable penalty factor strategy was proposed to ensure the model convergence [20]. However, the existing research often uses the traditional penalty factor strategy to minimize the difference between the optimization results of the MGs and the objectives provided by the SDN. Formulating appropriate penalty factor is difficult and the fast convergence of the optimization results cannot be guaranteed. The dual-side optimality of SDN-MGs is difficult to be obtained.

In a DG hosting capacity evaluation model, many constraints in the power grid must be taken into consideration, e.g., nonlinear power flow constraints. The node voltage and branch capacity are key factors limiting the development of renewable energy [21]. In addition, with the development of SDNs, ever-increasing amounts of flexible resources will need to be integrated into power systems in the future. This will lead to a sharp increase in the dimension of decision variables in the DG hosting capacity evaluation model. Getting the global optimal solution quickly has become a widespread concern of scholars. The optimal location and capacity of DG were achieved by genetic algorithm in [22]. An improved binary particle swarm optimization algorithm based on chaos optimization was proposed in [23]. However, many infeasible populations may be generated by the above intelligent algorithms. The power flow calculation must be repeated and the calculation speed was relatively low. In [24], the power flow equality constraints were relaxed into inequality constraints by second-order cone relaxation (SOCR); for a radial distribution network, the global optimality could be proven. Using SOCR, [25] relaxed non-convex power flow constraints and proposed a two-stage optimization solution method. Moreover, the active power, reactive power, and apparent capacity of ES and SOP can be modeled in the form of cone. Scholars are trying to model more devices into the form of cone.

In the future, there will be many flexible and adjustable resources such as ES and SOP in the SDN, which can improve the DG permeability. This means that their addition can improve the DG hosting capacity of SDN. Distributed ES can stabilize the fluctuation of DG output and improve the SDN flexibility [26]. The feasibility of DG construction with ES in an SDN in Brazil was evaluated in [27]. To make full use of rural rooftop solar resources, [28] improved the utilization efficiency of renewable energy through the coordinated planning of DG and distributed ES. A residential ES system was used in [29] to absorb PV peak output and reduce the peak-shaving pressure in an SDN. A centralized ES was utilized to stabilize the power fluctuations between a renewable energy station and the power grid in [30]. Both power supply costs and pollutants could be reduced. In addition, the advanced power electronic devices play an important role in the network [31], [32]. In terms of load, the matching degree between DG output and load demand could be improved by formulating a dynamic DR compensation scheme [33], [34]. Therefore, various flexible resources should be considered when evaluating the DG hosting capacity.

To sum up, existing research on DG hosting capacity evaluation methods in SDNs still has the following shortcomings.

1) The effects of multiple flexible resources on hosting capacity increase are not considered comprehensively, and the coordination action of ES and the curtailment of the DG peak output are ignored.

2) In the operation simulations of SDN-MGs, the MG operation privacy cannot be simply achieved by the centralized dispatching method. Furthermore, the distributed optimization methods based on penalty factors often have the problem of blindness in the selection of penalty factors.

In this paper, a quick hosting capacity evaluation method for SDN planning with DG is proposed. When evaluating the DG hosting capacity, the DG and distributed ES are integrated to SDN in the form of MG. A multi-objective DG hosting capacity evaluation model is established. The sub-cost value of the objective function is determined based on the sequential operation of SDN-MGs. To protect the MG operation privacy, a new distributed dispatching method is used to optimize the MG and SDN operation. And the dual-side optimal operation is realized through a few iterations of interactive power information on the upper limit of tie line. To decrease the calculation time for the optimal DG planning schemes, the steady-state security region (SSSR) of SDN is utilized to formulate the initial planning scheme. The highlights of this paper are as follows.

1) A multi-objective DG hosting capacity evaluation model is established. The DG hosting capacity of SDN is determined by the optimal DG planning schemes.

2) The SSSR is introduced to formulate the initial planning scheme of DGs to speed up the solving process.

3) The MG operation privacy is protected by the proposed distributed dispatching method. The dual-side optimal operation of SDN-MGs is realized through a few iterations to exchange the upper limit of power.

4) The DG hosting capacity is analyzed when the SDN is integrated with different flexible resources.

The rest of this paper is arranged as follows. Section II describes the optimization planning model of DG. Section III describes the calculation method for the system operation economic benefits based on distributed optimal dispatching. Section IV provides the hosting capacity evaluation results for DG in the SDN using the proposed method; for validation, it also makes a comparison with benchmark dispatching methods. Section V provides some conclusions of this paper.

II. Optimization Planning Model of DG

A. Multi-objective Optimization Planning Model

In the process of DG hosting capacity evaluation, the economic benefits and safe operation should be considered. From the perspective of economy, the equipment investment costs and the economic benefits from the system operation should be considered. The node voltages and branch currents should also be limited within the safe range.

1) Objective Function of DG Hosting Capacity Evaluation

It is assumed that there are N nodes in the SDN. The optimization objective of the hosting capacity evaluation model is obtaining the optimal installed capacity vector of PV $\boldsymbol{P}^{\mathrm{PV}}=[P_1^{\mathrm{PV}},P_2^{\mathrm{PV}},...,P_N^{\mathrm{PV}}]$ and the installed capacity vector of distributed ES $\boldsymbol{E}^{\mathrm{ES1}}=[E_1^{\mathrm{ES1}},E_2^{\mathrm{ES1}},...,E_N^{\mathrm{ES1}}]$.

2) Costs

The investment and maintenance costs of PV and distributed ES can be considered by the equal annual value method. The operation costs include the electricity purchase cost, electricity sale benefit, grid loss cost, compensation cost to DR users, and operation cost of centralized ES. The total cost C_{total} could be achieved by (1). The index of annual economic benefit, i.e., the opposite of C_{total}, is used later. For the DR, this paper considers the DR users of translational load [35]. The compensation cost C_4 can be calculated by multiplying the load shedding by the compensation price $C_{t,\text{DR}}$.

$$\begin{cases} C_{\text{total}} = C_1 + \sum_{day=1}^{365}\sum_{t=1}^{T}(C_2+C_3+C_4+C_5) \\ C_1 = (k_{\text{inv,PV}}+k_{\text{om,PV}})C_{\text{un,PV}}\sum_{i=1}^{N}P_i^{\text{PV}} + \\ \qquad (k_{\text{inv,ES1}}+k_{\text{om,ES1}})C_{\text{un,ES1}}\sum_{i=1}^{N}E_i^{\text{ES1}} \\ C_2 = (C_{t,\text{buy}}P_{t,\text{buy}}^{\text{tra}} - C_{t,\text{sell}}P_{t,\text{sell}}^{\text{tra}})\Delta t \\ C_3 = \sum_{ij\in E}\tilde{I}_{ij,t}r_{ij}C_t\Delta t \\ C_4 = C_{t,\text{DR}}\Delta t\sum_{i\in D}\left|P_{i,t}^{\text{load}} - P_{i,t}^{\text{ORG}}\right|/2 \\ C_5 = C_{\text{ES2}}\Delta t\sum_{i}\left|P_{i,t}^{\text{ES2}}\right| \end{cases} \tag{1}$$

3) Node Voltage Quality

Node voltage deviation should also be considered by the DSO. ΔU is introduced by:

$$\Delta U = \sum_{t=1}^{T}\sum_{i=1}^{N}\left|U_{i,t}-U_{i,\text{rate}}\right|\Delta t \tag{2}$$

Limited by the distribution of natural resources, the total installed capacity of PV can be denoted as:

$$P_{\text{PV}} = \sum_{i=1}^{N}P_i^{\text{PV}} \le P_{\max}^{\text{cap}} \tag{3}$$

where $P_{\max}^{\text{cap}}$ depends on the available land area, terrain, distribution of wind/solar resource, wind direction/solar radiation angle, and other factors of the project.

Economy and voltage quality should be considered comprehensively when planning distributed resources. However, only the equipment investment cost can be obtained directly according to the planning scheme of distributed resources. The remaining items should be obtained through sequential operation simulation, and the optimal planning scheme must be determined according to the simulation results.

B. Initial Planning Scheme

$\boldsymbol{P}^{\text{PV}}$ with high dimensions is a continuous variable. Compared with randomly generated methods, some inspired information can be used to generate better initial DG installed schemes. In this paper, the SSSR of SDN is introduced to solve the DG hosting capacity model quickly. The SSSR is used to describe the steady-state security constraints, e.g., node voltage constraints, in the form of region. The detailed formula derivation process could be found in [36]. Formula (4) describes the SSSR where the SDN can operate safely.

$$\Omega_{\text{SSSR}} \triangleq \left\{ \boldsymbol{x}_\beta \left| \sum_{i=1}^{N}(\alpha_{j,i}^{\text{V,M}}P_i+\beta_{j,i}^{\text{V,M}}Q_i)\le 1, \sum_{i=1}^{N}(\alpha_{j,i}^{\text{V,m}}P_i+\beta_{j,i}^{\text{V,m}}Q_i)\le 1, \right. \right. \\ \left. -1\le\sum_{i=1}^{N}(\alpha_{j,i}^{\text{I}}P_i+\beta_{j,i}^{\text{I}}Q_i)\le 1, P_i^{\text{m}}\le P_i\le P_i^{\text{M}}, Q_i^{\text{m}}\le Q_i\le Q_i^{\text{M}} \right\} \tag{4}$$

When no curtailment is allowed, the initial DG installation scheme is the minimum distance between the system operation point and the SSSR boundary. Constrained by the upper limit of voltage at node 1, the initial DG installed scheme of node i can be denoted as:

$$\Delta P_1^{i,\text{M}} = \begin{cases} \dfrac{1-\sum_{i=1}^{N}(\alpha_{1,i}^{\text{V,M}}P_i+\beta_{1,i}^{\text{V,M}}Q_i)}{\alpha_{1,i}^{\text{V,M}}} & \alpha_{1,i}^{\text{V,M}}>0 \\ +\infty & \alpha_{1,i}^{\text{V,M}}<0 \end{cases} \tag{5}$$

Constrained by the voltage operation range of N nodes in an SDN, the initial installed capacity of DG at node i can be similarly calculated, which are recorded as $\Delta P_1^{i,\text{M}}, \Delta P_1^{i,\text{m}}, \Delta P_2^{i,\text{M}}, \Delta P_2^{i,\text{m}}, \ldots, \Delta P_N^{i,\text{M}}, \Delta P_N^{i,\text{m}}$. Therefore, constrained by the upper and lower limits of all node voltages, the initial installed capacity of DG at node i can be calculated as:

$$\Delta P_{\text{V}}^{i} = \min\left\{\Delta P_1^{i,\text{M}}, \Delta P_1^{i,\text{m}}, \Delta P_2^{i,\text{M}}, \Delta P_2^{i,\text{m}}, \ldots, \Delta P_N^{i,\text{M}}, \Delta P_N^{i,\text{m}}\right\} \tag{6}$$

Similarly, constrained by the branch current limit, the initial installed capacity of DG at node i can be achieved, which is regarded as ΔP_{I}^{i}. To sum up, the initial DG installed scheme of node i can be determined by:

$$\Delta P_i^{\text{PV}} = \min\left\{\Delta P_{\text{V}}^{i}, \Delta P_{\text{I}}^{i}\right\} \tag{7}$$

During the normal operation of the SDN, the distributed ES is used to cut the peak and fill the valley, thereby improving the renewable energy permeability. The initial installed capacity of DG at node i $\Delta P_i^{\text{PV}\prime}$ considering distributed ES can be determined by the following model.

$$\min\sum_{t=1}^{T}\left(P_{i,t}^{\text{PV}} - \frac{1}{T}\sum_{t=1}^{T}P_{i,t,\max}^{\text{PV}}\right)^2 \tag{8}$$

s.t.

$$\begin{cases} E_{i,t+1}^{\text{ES1}} = E_{i,t}^{\text{ES1}} - (\eta_{\text{ES1,dis}}P_{i,t}^{\text{ES1,dis}} - \eta_{\text{ES1,cha}}P_{i,t}^{\text{ES1,cha}})\Delta t \\ k_{\text{soc,m1}}E_i^{\text{ES1}} \le E_{i,t}^{\text{ES1}} \le k_{\text{soc,M1}}E_i^{\text{ES1}} \\ 0\le P_{i,t}^{\text{ES1,dis}} \le P_{i,\max}^{\text{ES1}} \\ 0\le P_{i,t}^{\text{ES1,cha}} \le P_{i,\max}^{\text{ES1}} \\ P_{i,t}^{\text{ES1,cha}} - P_{i,t}^{\text{ES1,dis}} = P_{i,t,\max}^{\text{PV}} - P_{i,t}^{\text{PV}} \\ E_{i,1}^{\text{ES1}} = E_{i,\text{T}}^{\text{ES1}} \end{cases} \tag{9}$$

where $P_{i,t}^{\text{PV}}$ is gradually adjusted until the smoothed maximum PV output is equal to ΔP_i. The updated capacity of PV is $\Delta P_i^{\text{PV}\prime}$. Then, screen the grid integrated locations of DG, and allocate the capacity quota $P_{\max}^{\text{cap}}$ to these nodes. The vector $[\Delta P_1^{\text{PV}\prime}, \Delta P_2^{\text{PV}\prime}, \ldots, \Delta P_i^{\text{PV}\prime}, \ldots, \Delta P_N^{\text{PV}\prime}]$ can be obtained by calculating the initial DG installation schemes. The initial installed capacity of DG at node x in the SDN can be denoted as:

$$\Delta P_x = \frac{P_{\max}^{\text{cap}}\Delta P_x^{\text{PV}\prime}}{\sum_{i=1}^{N_{\text{int}}}\Delta P_i^{\text{PV}\prime}} \tag{10}$$

III. Calculation Method of System Operation Economic Benefit Based on Distributed Dispatching

A. Information Exchange Process in Distributed Dispatching Method

The control authority of distributed DG and ES belongs to the MG control centers. In contrast, the dispatching schemes of centralized ES and other equipment are determined by SDN DSO. The dispatching goal of the MG is to obtain the maximum economic benefit using time-of-use (TOU) price. The economic benefit and voltage quality are both considered by the DSO. The optimal operation of SDN-MGs can be realized by exchanging power upper limit information, as shown in Fig. 1.

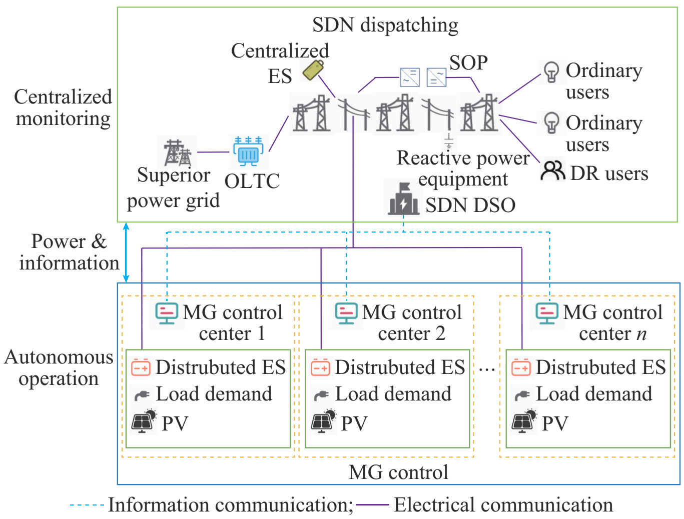

Fig. 1. Information exchange process in distributed dispatching.

The dual-side optimality of SDN-MGs can be achieved by exchanging the upper limits of tie line power. First, each MG control center formulates PV and ES dispatching schemes and reports the electricity purchase or sale requirements to the DSO. The optimization dispatching of SDN is then conducted according to the MG electricity purchase or sale schemes. The dispatching results for the upper limits of tie line power are transferred to all MG control centers. Finally, the MG control centers rearrange the ES and PV dispatching schemes based on the information from the DSO. After a few iterations, the final dispatching schemes are obtained. The convergence criterion is given as:

$$\sum_{t=1}^{T}\frac{\left|P_{i,t,\text{buy}}^{\text{net}}+P_{i,t,\text{sell}}^{\text{net}}-P_{i,t,\text{buy}}^{\text{line}}-P_{i,t,\text{sell}}^{\text{line}}\right|}{P_{i,t,\text{buy}}^{\text{net}}+P_{i,t,\text{sell}}^{\text{net}}}\leq\varepsilon \tag{11}$$

B. Optimization Dispatching Method of Distributed Resources

1) Optimization Dispatching Model of MG

Real-time electrical and information communication is established between the MGs and SDN. When the PV output is insufficient, the MG control center purchases electricity from the SDN and stores it in distributed ES. The optimization dispatching model of MG integrated into node i is shown in (12).

$$\begin{cases}\min\sum_{t=1}^{T}\Bigg[(C_{t,\text{buy}}P_{i,t,\text{buy}}^{\text{line}}-C_{t,\text{sell}}P_{i,t,\text{sell}}^{\text{line}})+C_{\text{ES1}}(P_{i,t}^{\text{ES1,dis}}+P_{i,t}^{\text{ES1,cha}})+\\ \left(C_{t,\text{buy}}\dfrac{(P_{i,t,\text{buy}}^{\text{line}})^2}{\tilde{U}_{i,t}}+C_{t,\text{sell}}\dfrac{(P_{i,t,\text{sell}}^{\text{line}})^2}{\tilde{U}_{i,t}}\right)R\Bigg]\Delta t\\ \text{s.t. (9)}\\ P_{i,t,\text{buy}}^{\text{line}}-P_{i,t,\text{sell}}^{\text{line}}=P_{i,t}^{\text{load}}-P_{i,t}^{\text{PV}}-P_{i,t}^{\text{ES1}}\\ 0\leq P_{i,t,\text{buy}}^{\text{line}}\leq\alpha_1 P_{i,t,\text{sell}}^{\text{net}}\\ 0\leq P_{i,t,\text{sell}}^{\text{line}}\leq\alpha_2 P_{i,t,\text{buy}}^{\text{net}}\\ 0\leq\alpha_1+\alpha_2\leq 1\end{cases} \tag{12}$$

In the above optimization dispatching model, the target is minimizing the electricity purchase cost, the distributed ES operation cost, and the power loss on the tie line, and maximizing the economic profit of selling electricity. Aiming at the balance constraints of tie line power, it should be noted that electricity cannot be purchased and sold at the same time [37]. The operation constraints of distributed ES must be considered.

2) Optimization Dispatching Model of SDN

In this subsection, the optimization planning objectives of distributed resources are analyzed in detail. The equipment investment cost, electricity purchase cost, electricity sale benefit, grid loss cost, compensation cost to DR user, operation cost of centralized ES, and node voltage quality are comprehensively considered. The objective function can be obtained through sequential operation simulation, except for equipment investment cost. Therefore, the dispatching objective function of the SDN is denoted as:

$$\min[k_1(C_2+C_3+C_4+C_5)+k_2\Delta U] \tag{13}$$

The basic active and reactive power balance should be met, as given by:

$$P_{i,t,\text{sell}}^{\text{net}}-P_{i,t,\text{buy}}^{\text{net}}-P_{i,t}^{\text{ES2}}=P_{ji,t}+\sum_{m\in S(i)}P_{mi,t}^{\text{SOP}}-r_{ij}\tilde{I}_{ij,t}-\sum_{k\in H(i)}P_{ik,t}-P_{i,t}^{\text{load}} \tag{14}$$

$$Q_{i,t}^{\text{load}}-Q_{i,t}^{\text{ES2}}-Q_{i,t}^{\text{C}}-Q_{i,t}^{\text{SVG}}=Q_{ji,t}+\sum_{m\in S(i)}Q_{mi,t}^{\text{SOP}}-x_{ij}\tilde{I}_{ij,t}-\sum_{k\in H(i)}Q_{ik,t} \tag{15}$$

The voltages of adjacent nodes should satisfy the voltage drop constraint, which is given as:

$$\tilde{U}_{j,t}=\tilde{U}_{i,t}-2(r_{ij}P_{ij,t}+x_{ij}Q_{ij,t})+(r_{ij}^2+x_{ij}^2)\tilde{I}_{ij,t} \tag{16}$$

The branch currents and node voltages should be limited within the safe range:

$$\begin{cases}\tilde{I}_{ij,t}\leq I_{ij,\max}^2\\ U_{i,\min}^2\leq\tilde{U}_{i,t}\leq U_{i,\max}^2\end{cases} \tag{17}$$

The relationship among branch currents, node voltages, and branch active and reactive power can be denoted as:

$$\left\|[2P_{ij,t}\quad 2Q_{ij,t}\quad \tilde{I}_{ij,t}-\tilde{U}_{i,t}]^{\text{T}}\right\|_2\leq\tilde{I}_{ij,t}+\tilde{U}_{i,t} \tag{18}$$

The apparent capacity and the active and reactive power of SOP meet the following cone formula.

$$\left\|\left[P_{mi,t}^{\text{SOP}}\quad Q_{mi,t}^{\text{SOP}}\right]^{\text{T}}\right\|_2\leq S_i^{\text{SOP}} \tag{19}$$

When the SDN DSO lays down the upper limits of power information, the load demand of the MGs should be satisfied as far as possible. The exchange power of the SDN and MGs should meet the following constraints.

$$\begin{cases} 0 \le P_{i,t,\text{sell}}^{\text{net}} \le P_{i,t,\text{buy}}^{\text{line}} \\ 0 \le P_{i,t,\text{buy}}^{\text{net}} \le P_{i,t,\text{sell}}^{\text{line}} \end{cases} \tag{20}$$

The DSO can purchase electricity from or sell electricity to the higher-voltage power grid through a transformer. The exchanged power limits of the SDN and the superior grid can be denoted as:

$$\begin{cases} 0 \le P_{t,\text{buy}}^{\text{tra}} \le \beta_1 P_{\max,\text{buy}}^{\text{tra}} \\ 0 \le P_{t,\text{sell}}^{\text{tra}} \le \beta_2 P_{\max,\text{sell}}^{\text{tra}} \\ 0 \le \beta_1 + \beta_2 \le 1 \end{cases} \tag{21}$$

The root node voltage is determined by on-load tap changer (OLTC). Assuming that OLTC has s gears, the root node voltage meets the following constraints.

$$\begin{cases} k_{\min} \le k_t \le k_{\max} \\ k_t = k_{\min} + \sum_s k_s \gamma_{s,t}^{\text{OLTC}} \\ U_{0,t}^2 = k_t U_{0,\text{rate}}^2 \end{cases} \tag{22}$$

Static var generator (SVG) can be adjusted continuously and can absorb reactive power or emit reactive power. The operation constraints of SVG are given by:

$$-Q_{i,\max}^{\text{SVG}} \le Q_{i,t}^{\text{SVG}} \le Q_{i,\max}^{\text{SVG}} \tag{23}$$

The reactive power output of capacitor bank (CB) is related to the number of input groups, and there is an upper limit of changing time during a dispatching period. The operation constraints of CB are given by:

$$\begin{cases} Q_{i,t}^{\text{C}} = n_{i,t}^{\text{C}} Q_i^C \\ n_{i,\min}^{\text{C}} \le n_{i,t}^{\text{C}} \le n_{i,\max}^{\text{C}} \\ n_{i,t}^{\text{C}} - n_{i,t-1}^{\text{C}} \le (n_{i,\max}^{\text{C}} - n_{i,\min}^{\text{C}}) b_{i,t} \\ n_{i,t-1}^{\text{C}} - n_{i,t}^{\text{C}} \le (n_{i,\max}^{\text{C}} - n_{i,\min}^{\text{C}}) b_{i,t} \\ \sum_{t=1}^{T} b_{i,t} \le \lambda_{\text{C}} \end{cases} \tag{24}$$

There is electricity loss during the charging and discharging of ES. However, the ES control technology is becoming increasingly mature, and ES reactive power should also be considered, as given by:

$$\begin{cases} -Q_{i,\max}^{\text{ES2}} \le Q_{i,t}^{\text{ES2}} \le Q_{i,\max}^{\text{ES2}} \\ \sqrt{(P_{i,t}^{\text{ES2}})^2 + (Q_{i,t}^{\text{ES2}})^2} \le S_i^{\text{ES2}} \\ \sqrt{(P_{i,t}^{\text{ES2}})^2 + (Q_{i,t}^{\text{ES2}})^2} \le \dfrac{E_{i,t}^{\text{ES2},1}}{\eta_i} \\ E_{i,t+1}^{\text{ES2}} = E_{i,t}^{\text{ES2}} - (E_{i,t}^{\text{ES2},1} + P_{i,t}^{\text{ES2}}) \Delta t \\ k_{\text{soc},\text{m2}} E_i^{\text{ES2}} \le E_{i,t}^{\text{ES2}} \le k_{\text{soc},\text{M2}} E_i^{\text{ES2}} \\ E_{i,1}^{\text{ES2}} = E_{i,T}^{\text{ES2}} \end{cases} \tag{25}$$

The total power consumption of DR users during one dispatching period remains unchanged. Relevant constraints are given by:

$$\begin{cases} \sum_{t=1}^{T} P_{i,t}^{\text{load}} = \sum_{t=1}^{T} P_{i,t}^{\text{ORG}} \\ d_1 P_{i,t}^{\text{ORG}} \le P_{i,t}^{\text{load}} \le d_2 P_{i,t}^{\text{ORG}} \end{cases} \tag{26}$$

Formula (27) is used to calculate the node voltage deviation of the SDN.

$$\begin{cases} u_{i,t} \ge 0 \\ u_{i,t} \ge \tilde{U}_{i,t} - U_{i,\min}^2 \\ u_{i,t} \ge -\tilde{U}_{i,t} + U_{i,\max}^2 \end{cases} \tag{27}$$

The following optimization dispatching model of SDN is established as (28). The flow chart of specific distributed resource planning is shown in Fig. 2. Both k_1 and k_2 used in the SDN dispatching model are 0.5.

$$\begin{cases} \min[k_1(C_2 + C_3 + C_4 + C_5) + k_2 \Delta U] \\ \text{s.t. (14)-(27)} \end{cases} \tag{28}$$

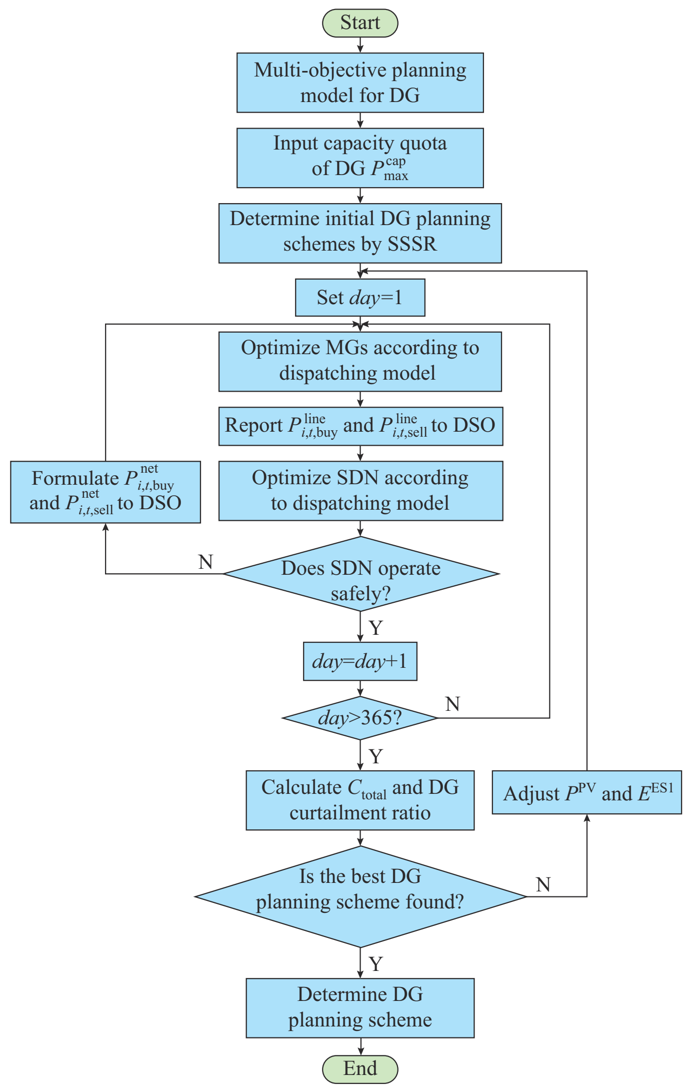

Fig. 2. Flow chart of distributed resource planning.

IV. Case Study

A. Simulation Background

This subsection analyzes the IEEE 33-bus system with four MGs, as shown in Fig. 3. An MG is composed of distributed PV and ES. Centralized ES and other equipment are integrated into a traditional distribution network. Nodes 23 and 6 are equipped with translational loads, and all traditional interconnection switches are replaced with SOPs. The MGs to be built are located at nodes 4, 9, 15, and 31. The capacity of distributed ES in each MG is 20% of DG. The distributed ES has a 0.5C charging or discharging ability, the loss coefficient is 0.02, and the initial state of charge (SOC) is 0.5. The investment costs of distributed PV and ES are 4 ¥/kW and 2 ¥/kW, respectively. The centralized ES invested by the SDN is located at node 29. This could store up to 3 MWh; and the loss coefficient is 0.02 and the apparent capacity is 3 MVA. The maximum reactive power output is 600 kvar, and the initial electricity quantity is 500 kWh. C_{ES1} and C_{ES2} are both 0.2 ¥/kWh. The capacities of CB at nodes 2 and 24 are both 10×50 kvar. An SVG is located at node 15 and its maximum adjustable range of reactive power is [−1,−1]Mvar. The rated capacity of the line is 5 MVA. The safe range of node voltage is [0.95, 1.05]p.u.. The apparent capacity of SOP is 1.5 MVA. The TOU price is shown in Fig. 4.

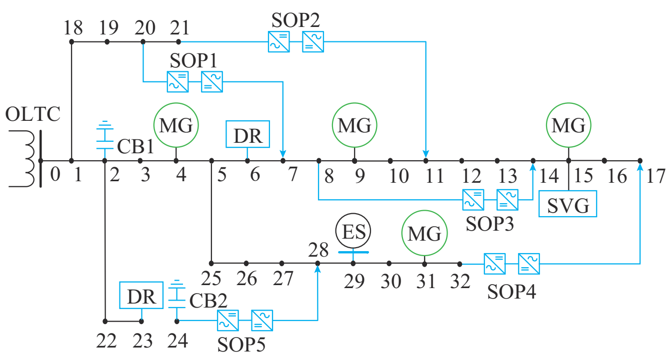

Fig. 3. IEEE 33-bus system with four MGs.

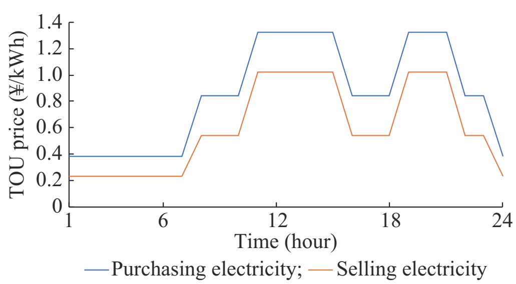

Fig. 4. TOU price.

B. Analysis of MG Planning Schemes

1) Initial Planning Schemes

According to Section II, the initial PV planning scheme can be obtained based on the distance between the current operation point and SSSR boundary. The initial PV planning schemes can be directly affected by the current system operation point. When the largest ratio operation point corresponding to the initial PV planning schemes is selected, the installed capacity proportion of DG at the four nodes can be obtained. The main function of ES is smoothing PV output fluctuation. Therefore, the installed capacity proportion of DG is different from the initial capacity information directly obtained by SSSR when ES is considered. The initial DG planning schemes are given in Table I.

TABLE I
INITIAL DG PLANNING SCHEMES

P_{max}^{cap} (MW)	P_4^{PV} (kW)	P_9^{PV} (kW)	P_{15}^{PV} (kW)	P_{31}^{PV} (kW)
14	6575	3050	1725	2650
16	7525	3475	1980	3020
18	8450	3900	2250	3400
20	9400	4350	2500	3750
22	10350	4775	2725	4150
24	11300	5200	2970	4530
26	12225	5650	3225	4900
28	13175	6080	3465	5280
30	14100	6525	3700	5675

2) Analysis of Dispatching Schemes on a Typical Day

1) Dispatching schemes on a typical day

When P^{PV} is 20 MW, a day-ahead economic dispatch is performed according to the initial DG planning schemes in Table I, following the distributed optimal dispatching method in this paper. First, the MGs optimize and report the electricity interaction requirement to the DSO. In the first optimization of the MG at node 9, the upper limit of power interaction scheme is the rated capacity of tie line, i.e., 5000 kW, as shown by the blue bars in Fig. 5(a).

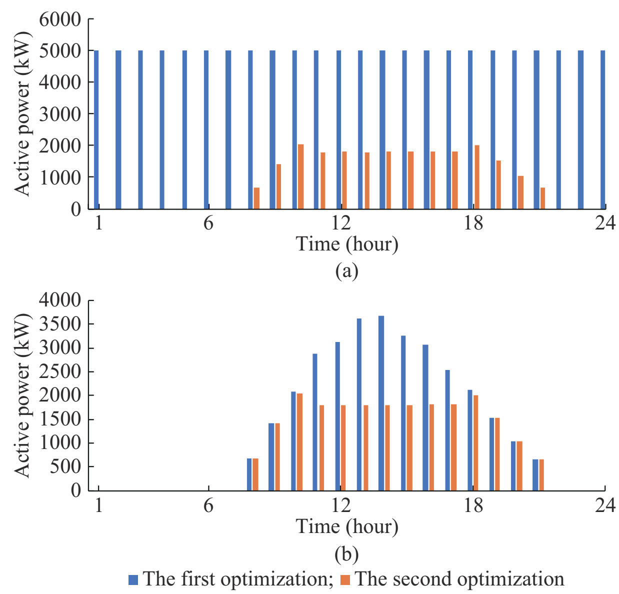

Fig. 5. The upper limit of exchange power between MG and SDN. (a) The upper limit of power sold by MG at node 9. (b) The upper limit of power purchased by SDN from MG at node 9.

Then, the DSO verifies whether the reported electricity interaction requirement, as shown by the blue bars in Fig. 5(b), can be satisfied under security operation constraints. As shown in Fig. 6(a), the node voltage exceeds the limit, which is especially obvious during the noon period. Therefore, not all the electricity interaction requirement can be fully satisfied. It is necessary to reasonably curtail some PV output. With (28), the DSO determines and passes the upper limits of tie line power, as shown by the orange bars in Fig. 5(a), to the MG at node 9.

After obtaining the upper limit of power, the MG at node 9 reconducts the day-ahead optimization with (12). A new electricity interaction requirement is obtained and reported to the DSO again. The DSO repeats the above verification and gets the orange bars in Fig. 5(b). Iterative calculation is conducted according to the above logic until (11) is met. The final power upper limits of each MG emitted by the DSO are shown in Table II. So far, the node voltage distribution in Fig. 6(b) can be achieved.

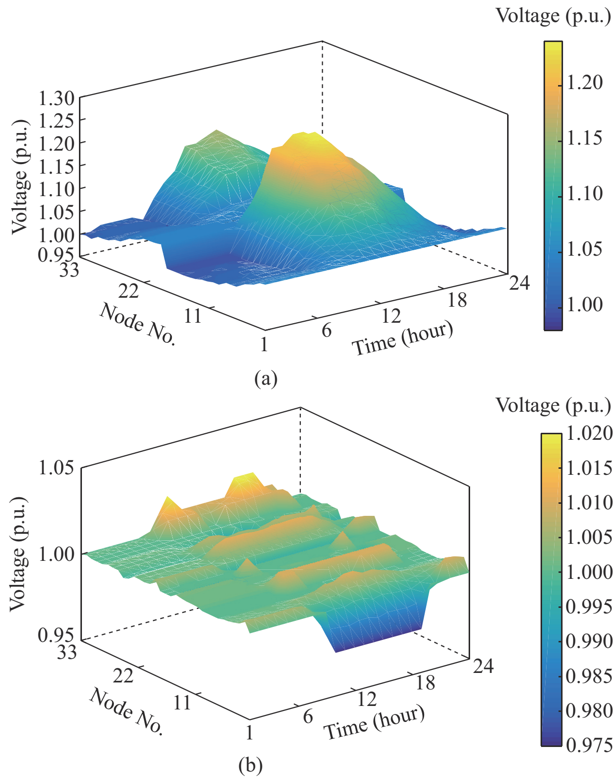

Fig. 6. Node voltage distribution under different conditions. (a) Node voltage distribution when electricity sale wishes of all MGs are met. (b) Node voltage distribution when the upper power limits are modified.

TABLE II
FINAL POWER UPPER LIMITS

Time	$P^{net}_{4,t,buy}$ (kW)	$P^{net}_{9,t,buy}$ (kW)	$P^{net}_{15,t,buy}$ (kW)	$P^{net}_{31,t,buy}$ (kW)
00:00-09:00	-	-	-	-
09:00-10:00	-	2041	894	1386
10:00-11:00	-	1793	541	1199
11:00-12:00	-	1798	544	1201
12:00-13:00	-	1793	541	1199
13:00-14:00	-	1798	544	1201
14:00-15:00	-	1798	544	1201
15:00-16:00	-	1823	883	1547
16:00-17:00	-	1808	885	1547
17:00-18:00	-	2013	894	1409
18:00-24:00	-	-	-	-

The final dispatching schemes of all MGs are shown in Fig. 7. The initial electricity purchase or sale schemes formulated by the MG at node 4 are satisfied and $P^{net}_{4,t,buy}$ is not limited. However, $P^{net}_{9,t,buy}$, $P^{net}_{15,t,buy}$, and $P^{net}_{31,t,buy}$ are limited due to their different installation locations. The electricity exchange plan between the SDN and superior grid, and the root node voltage are shown in Fig. 8.

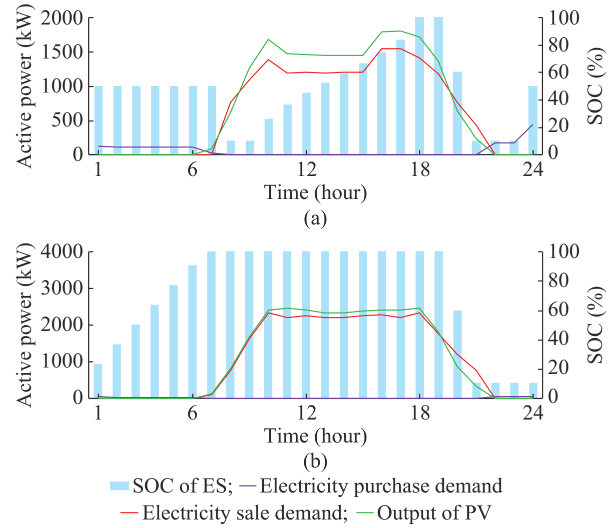

Fig. 7. Final dispatching schemes of MGs. (a) Final dispatching scheme of node 4. (b) Final dispatching scheme of node 9.

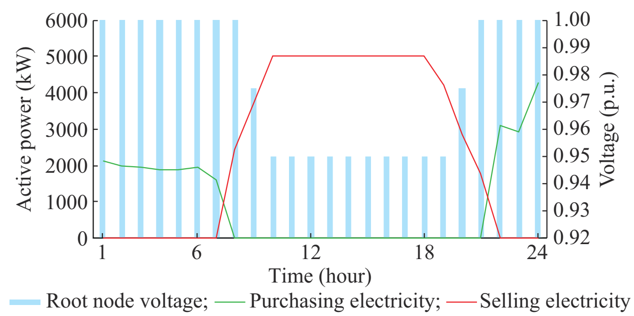

Fig. 8. Electricity exchange plan between SDN and superior grid, and root node voltage.

2) Comparison of dispatching methods

The proposed distributed dispatching method is compared with centralized and independent dispatching methods. In the centralized dispatching method, all equipment of MGs and SDN is regarded as a whole. In the independent dispatching method, MGs and SDN optimize themselves and there is no adjustment based on information exchange. The daily economic benefits obtained by the three dispatching methods are shown in Fig. 9.

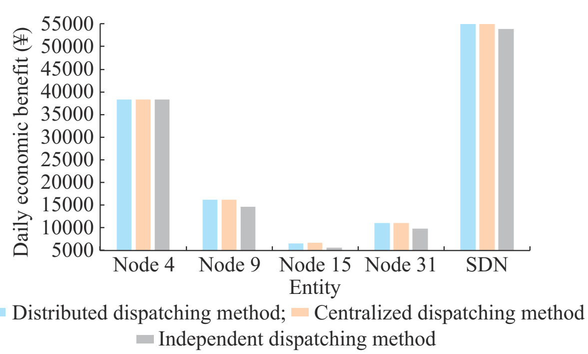

Fig. 9. Daily economic benefits of different entities by selling electricity.

Usually, the centralized dispatching method could obtain the best solution and is regarded as the benchmark. The difference between the economic benefits obtained by the distributed and centralized dispatching methods is within 1%. Therefore, the proposed distributed dispatching method could realize the dual-side optimality of SDN-MGs. While, there is an obvious gap between the economic benefits obtained by the independent dispatching method and others.

Compared with commonly used intelligent algorithm, a lot of power flow calculations can be avoided by the proposed SOCR solving method. An intelligent harmony search (HS) algorithm in [38], [39] is used as the comparison algorithm. The size of the harmony library is 50, the probability of taking value from harmony library is 0.5, the fine-tuning probability is 0.2, and the number of creations is 200. The total DG consumption rate during the whole dispatching period obtained by SOCR is obviously higher than that obtained by the HS algorithm, as shown in Table III. The calculation time of HS algorithm is much longer than that of SOCR method.

TABLE III
CALCULATION EFFECT COMPARISON

Algorithm	DG consumption rate (%)	Calculation time (s)
SOCR	71.53	42.47
HS	58.27	368.52

3) Optimization Planning Schemes Based on Equal Curtailment Ratio Principle

When P^{PV} is 20 MW, the PV planning schemes can be formulated by the distributed dispatching method and the equal curtailment ratio principle. According to the method in this paper, the PV installed schemes can be obtained by gradually adjusting the installed capacity of PV at four nodes until the equal curtailment ratio is met. Table IV provides the optimization process of installed capacity schemes for PV. The initial and optimal installed capacities of PV at each node are shown in Fig. 10. The final PV installed schemes are close to the initial one. It is found that the SSSR of SDN provides good heuristic information.

The optimal installed capacities of PV with different P_{max}^{cap} are obtained according to the above planning method based on the equal curtailment ratio principle, as shown in Table V. The changing trends in annual economic benefits, considering the continuous progress of renewable power technologies and the continuous decrease in equipment prices, are shown in Fig. 11. The scatter under three different equipment costs (costs A, B, C) is fitted quadratically. The changing trends in annual economic benefits are well reflected by the fitting curve. The following three points are found.

1) The annual economic benefits and the permeability of PV capacity can be improved by allowing a part of PV output to be curtailed.

2) The optimal installed capacity of DG in each MG and P^{PV} are not immutable, and dynamic optimization planning should be conducted in the future.

3) With the decrease in equipment investment costs, P^{PV} is increasing.

TABLE IV
OPTIMIZATION PROCESS OF INSTALLED CAPACITY SCHEMES FOR PV

Node i	P_i^{PV} (kW)	Curtailment ratio (%)
$i=4$	9600	9.54
	10000	12.11
	10500	14.18
	11700	19.18
	11800	19.58
	11830	19.68
$i=9$	4340	25.81
	4150	25.10
	4000	24.38
	3550	20.03
	3550	20.03
	3520	19.72
$i=15$	2274	34.93
	2300	32.84
	2100	29.68
	1600	19.55
	1650	20.56
	1600	19.63
$i=31$	3776	27.38
	3550	25.61
	3400	24.18
	3150	21.03
	3000	19.09
	3050	19.68

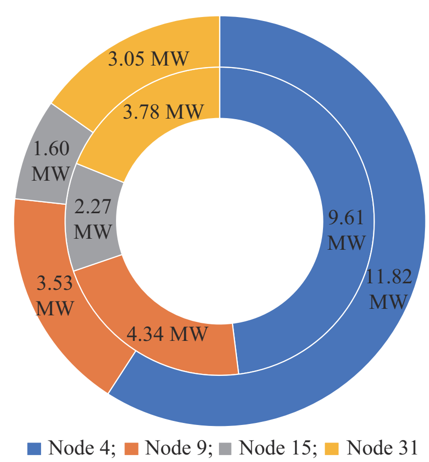

Fig. 10. Initial and optimal installed capacities of PV at each node.

C. Influence Analysis of Distributed ES and Other Resources

1) Influence of Distributed ES Capacity

Increasing ES capacity can reduce the DG curtailment ratio, but it will simultaneously lead to an increase in investment costs. Taking $P^{PV}=20$ MW as an example, the PV curtailment ratio and annual economic benefits are recorded, as shown in Fig. 12. The scatter is fitted quadratically, and the determination coefficient R^2 is 0.9988. It shows that the optimal total installed capacity of distributed ES is 2.83 MW, and the annual economic benefit is ￥2.82×10^6. With the development in the distributed ES, the PV curtailment ratio gradually decreases. Moreover, an increasing ES capacity can improve the annual economic benefit of SDN, and there is an optimal installed capacity.

TABLE V
OPTIMAL INSTALLED CAPACITY OF PV WITH DIFFERENT P_{max}^{cap}

P_{max}^{cap} (MW)	P_4^{PV} (kW)	P_9^{PV} (kW)	P_{15}^{PV} (kW)	P_{31}^{PV} (kW)
14	8120	2425	1115	2340
16	9350	2810	1270	2570
18	10550	3200	1425	2825
20	11825	3525	1600	3050
22	13010	3845	1825	3320
24	14210	4200	1970	3620
26	15410	4540	2130	3920
28	16625	4880	2295	4200
30	17855	5200	2485	4460

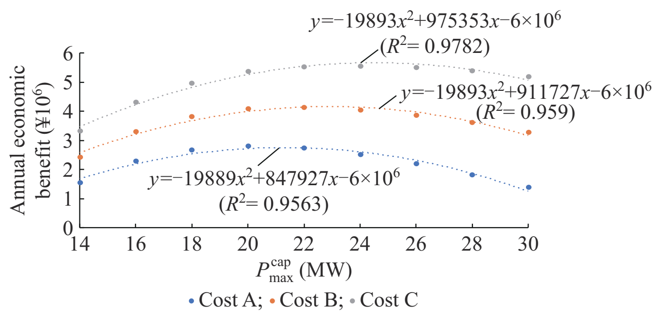

Fig. 11. Changing trends in annual economic benefits.

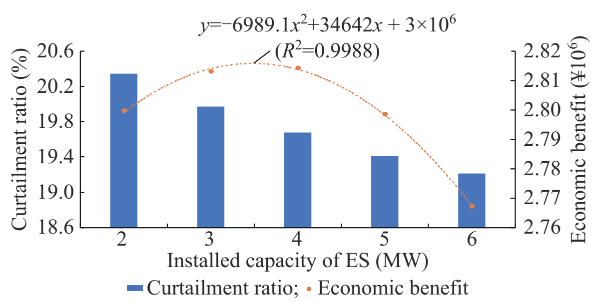

Fig. 12. Changing trends for economic benefits and PV curtailment ratio.

2) *Planning Schemes in Different Scenarios*

The following four scenarios are established for comparison to verify the promotion effect of flexible resources on DG planning and consumption. ① Scenario 1: DG planning considering the source-grid-load-storage resources. ② Scenario 2: DG planning considering the source-load-storage resources. ③ Scenario 3: DG planning considering the source-grid-storage resources. ④ Scenario 4: DG planning considering the source-grid-load resources. In the above four scenarios, the storage resources only refer to the centralized ES invested by the SDN. The optimal DG planning schemes in the above four scenarios, when $P^{PV}=20$ MW, are shown in Fig. 13. The PV curtailment ratio and the annual economic benefits are shown in Table VI. In Scenario 1, with the same ES installed capacity, the PV curtailment ratio can be minimized. Compared with Scenario 2, the PV curtailment ratio is reduced by 8.78% and the annual economic benefit is improved by ¥4.02×10^6. All types of flexible resources can reduce the PV curtailment ratio and improve the annual economic benefits. Among them, SOPs have a significant impact on the optimal DG planning schemes. SOPs can affect the decision of whether a DG unit should be installed at node 9. SOPs can make the power flow direction more flexible, and make better use of the wind and PV resources within the power supply range. Therefore, the impact of SOP on the DG planning schemes should be fully considered.

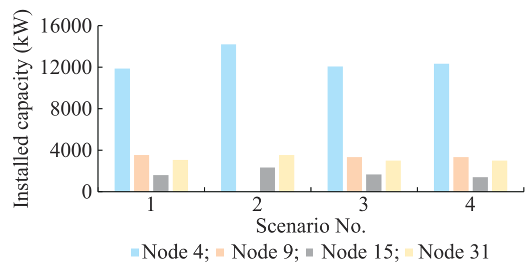

Fig. 13. Optimal DG planning schemes in four scenarios.

TABLE VI
PV CURTAILMENT RATIOS AND ANNUAL ECONOMIC BENEFITS

Scenario No.	PV curtailment ratio (%)					Annual economic benefit (¥10^6)
	Node 4	Node 9	Node 15	Node 31	Total	
1	19.68	19.71	19.63	19.68	19.68	2.81
2	28.57	-	28.38	28.42	28.46	1.21
3	20.95	20.98	20.90	21.01	20.96	2.37
4	22.10	22.33	21.96	22.32	22.17	1.40

V. CONCLUSION

A quick hosting capacity evaluation method for SDN planning with DG is proposed in the paper. A multi-objective DG hosting capacity evaluation model is established and the hosting capacity can be achieved by the optimal planning schemes of DG and distributed ES. The SSSR method is used to formulate the initial planning schemes skillfully. Distributed dispatching method is proposed to realize dual-side optimal operation of the SDN-MGs. The DG hosting capacity is analyzed when the SDN is integrated with different flexible resources. Based on the quick hosting capacity evaluation method, an SDN with four MGs is analyzed. The following results are found.

1) With the initial DG planning scheme obtained by the SSSR method, the optimal DG planning scheme can be obtained by only several adjustments (6 times in this paper). The evaluation speed of hosting capacity is accelerated greatly.

2) Without obvious sacrifice of calculation accuracy and speed, the proposed distributed dispatching method can realize dual-side optimal operation of SDN-MGs.

3) The DG hosting capacity of SDN could exceed the sum of the maximum active power demand and the rated branch capacity. The annual DG electricity could exceed the annual load demand.

4) With the decrease in equipment prices, the optimal DG

installed capacity is rising. It is necessary to dynamically evaluate the DG hosting capacity in the future.

REFERENCES

[1] J. Li, C. Gu, Y. Xiang *et al*., "Edge-cloud computing systems for smart grid: state-of-the-art, architecture, and applications," *Journal of Modern Power Systems and Clean Energy*, vol. 10, no. 4, pp. 805-817, Jul. 2022.

[2] O. Jogunola, B. Adebisi, K. Anoh *et al*., "Multi-commodity optimization of peer-to-peer energy trading resources in smart grid," *Journal of Modern Power Systems and Clean Energy*, vol. 10, no. 1, pp. 29-39, Jan. 2022.

[3] C. Bai, Q. Li, W. Zhou *et al*., "Fast distributed gradient descent method for economic dispatch of microgrids via upper bounds of second derivatives," *Energy Reports*, vol. 8, pp. 1051-1060, Aug. 2022.

[4] K. Wu, Q. Li, Z. Chen *et al*., "Distributed optimization method with weighted gradients for economic dispatch problem of multi-microgrid systems," *Energy*, vol. 222, p. 119898, May 2021.

[5] V. Püvi and M. Lehtonen. "Evaluating distribution network optimal structure with respect to solar hosting capacity," *Electric Power Systems Research*, vol. 216, p. 109019, Mar. 2023.

[6] M. S. S. Abad and J. Ma. "Photovoltaic hosting capacity sensitivity to active distribution network management," *IEEE Transactions on Power Systems*, vol. 36, no. 1, pp. 107-117, Jan. 2021.

[7] X. Xu, D. Niu, L. Peng *et al*., "Hierarchical multi-objective optimal planning model of active distribution network considering distributed generation and demand-side response," *Sustainable Energy Technologies and Assessments*, vol. 53, p. 102438, Oct. 2022.

[8] H. Wu, Y. Yuan, X. Zhang *et al*., "Robust comprehensive PV hosting capacity assessment model for active distribution networks with spatiotemporal correlation," *Applied Energy*, vol. 323, p. 119558, Oct. 2022.

[9] J. Guo, Z. Liu, X. Wu *et al*., "Two-layer co-optimization method for a distributed energy system combining multiple energy storages," *Applied Energy*, vol. 322, p. 119486, Sept. 2022.

[10] L. Ge, H. Liu, J. Yan *et al*., "Optimal integrated energy system planning with dg uncertainty affine model and carbon emissions charges," *IEEE Transactions on Sustainable Energy*, vol. 13, no. 2, pp. 905-918, Apr. 2022.

[11] B. Sun, Y. Li, Y. Zeng *et al*., "Distribution transformer cluster flexible dispatching method based on discrete monkey algorithm," *Energy Reports*, vol. 7, pp. 1930-1942, Nov. 2021.

[12] J. Liu, Y. Chen, C. Duan *et al*., "Distributionally robust optimal reactive power dispatch with Wasserstein distance in active distribution network," *Journal of Modern Power Systems and Clean Energy*, vol. 8, no. 3, pp. 426-436, May 2020.

[13] Y. Xu and J. Zhang. "A two-layer two-stage dispatching strategy for active distribution network with micro-grid considering multiple interactions," *Electric Power Systems Research*, vol. 187, p. 106504, Oct. 2020.

[14] W. Ma, J. Wang, V. Gupta *et al*., "Distributed energy management for networked microgrids using online ADMM with regret," *IEEE Transactions on Smart Grid*, vol. 9, no. 2, pp. 847-856, Jun. 2018.

[15] H. J. Gao, J. Liu, L. Wang *et al*., "Decentralized energy management for networked microgrids in future distribution systems," *IEEE Transactions on Power Systems*, vol. 33, no. 4, pp. 3599-3610, Nov. 2018.

[16] X. Zhu, J. Yang, X. Zhan *et al*., "Cloud-edge collaborative distributed optimal dispatching strategy for an electric-gas integrated energy system considering carbon emission reductions," *International Journal of Electrical Power & Energy Systems*, vol. 143, p. 108458, Dec. 2022.

[17] S. Ullah, L. Khan, I. Sami *et al*., "Voltage/frequency regulation with optimal load dispatch in microgrids using SMC based distributed cooperative control," *IEEE Access*, vol. 10, pp. 64873-64889, Jun. 2022.

[18] W. Zheng, Y. Hou, and Z. Li, "A dynamic equivalent model for district heating networks: formulation, existence and application in distributed electricity-heat operation," *IEEE Transactions on Smart Grid*, vol. 12, pp. 2685-2695, May 2021.

[19] P. Du, Z. Chen, Y. Chen *et al*., "A bi-level linearized dispatching model of active distribution network with multi-stakeholder participation based on analytical target cascading," *IEEE Access*, vol. 7, pp. 154844-154858, Oct. 2019.

[20] J. Chen, Z. Lin, J. Ren *et al*., "Distributed multi-scenario optimal sizing of integrated electricity and gas system based on ADMM," *Energy Systems*, vol. 117, p. 105675, May 2022.

[21] Kouveliotis-Lysikatos, N. Hatziargyriou, Y. Liu *et al*., "Towards an internet-like power grid," *Journal of Modern Power Systems and Clean Energy*, vol. 10, no. 1, pp. 1-11, Jan. 2022.

[22] P. Cortés, J. Muñuzuri, M. Berrocal-de-O *et al*., "Genetic algorithms to optimize the operating costs of electricity and heating networks in buildings considering distributed energy generation and storage," *Computers & Operations Research*, vol. 96, pp. 157-172, Aug. 2018.

[23] Y. Li, B. Feng, B. Wang *et al*., "Joint planning of distributed generations and energy storage in active distribution networks: a bi-level programming approach," *Energy*, vol. 245, p. 123226, Apr. 2022.

[24] M. Farivar and S. H. Low, "Branch flow model: relaxations and convexification-Part I," *IEEE Transactions on Power Systems*, vol. 28, no. 3, pp. 2554-2564, Aug. 2013.

[25] T. Ding, S. Liu, Z. Wu *et al*., "Sensitivity-based relaxation and decomposition method to dynamic reactive power optimisation considering DGs in active distribution networks," *IET Generation*, *Transmission & Distribution*, vol. 11, no. 1, pp. 37-48, Jan. 2017.

[26] C. Wang, L. Zhang, K. Zhang *et al*., "Distributed energy storage planning considering reactive power output of energy storage and photovoltaic," *Energy Reports*, vol. 8, pp. 562-569, Nov. 2022.

[27] G. N. D. Doile, P. R. Junior, L. C. S. Rocha *et al*., "Feasibility of hybrid wind and photovoltaic distributed generation and battery energy storage systems under techno-economic regulation," *Energy Reports*, vol. 195, pp. 1310-1323, Aug. 2022.

[28] H. Yuan, H. Ye, Y. Chen *et al*., "Research on the optimal configuration of photovoltaic and energy storage in rural microgrid," *Energy Reports*, vol. 8, no. 13, pp. 1285-1293, Nov. 2022.

[29] H. S. Zhou, R. Passey, A. Bruce *et al*., "Impact of residential battery energy storage systems on the peak reverse power flows from distributed photovoltaic systems," *Journal of Energy Storage*, vol. 52, p. 104817, Aug. 2022.

[30] M. Eslahi, A. F. Nematollahi, B. Vahidi *et al*., "Day-ahead scheduling of centralized energy storage system in electrical networks by proposed stochastic MILP-based bi-objective optimization approach," *Electric Power Systems Research*, vol. 192, p. 106915, Mar. 2021.

[31] P. Li, H. Ji, C. Wang *et al*., "Coordinated control method of voltage and reactive power for active distribution networks based on soft open point," *IEEE Transactions on Sustainable Energy*, vol. 8, pp. 1430-1442, Oct. 2017.

[32] L. Bai, T. Jiang, F. Li *et al*., "Distributed energy storage planning in soft open point based active distribution networks incorporating network reconfiguration and DG reactive power capability," *Applied Energy*, vol. 210, pp. 1082-1091, Jan. 2018.

[33] Q. Cai, Q. Xu, J. Qing *et al*., "Promoting wind and photovoltaics renewable energy integration through demand response: dynamic pricing mechanism design and economic analysis for smart residential communities," *Energy*, vol. 261, p. 125293, Dec. 2022.

[34] X. Zhao, Z. Bai, W. Xue *et al*., "Research on bi-level cooperative robust planning of distributed renewable energy in distribution networks considering demand response and uncertainty," *Energy Reports*, vol. 7, pp. 1025-1037, Nov. 2021.

[35] B. Sun, R. Jing, Y. Zeng *et al*., "Distributed optimal dispatching method for smart distribution network considering effective interaction of source-network-load-storage flexible resources," *Energy Reports*, vol. 9, pp. 148-162, Dec. 2023.

[36] T. Yang and Y. Yu. "Static voltage security region-based coordinated voltage control in smart distribution grids," *IEEE Transactions on Smart Grid*, vol. 9, no. 6, pp. 5494-5502, Nov. 2018.

[37] B. Sun, R. Jing, Y. Zeng *et al*., "Distributed optimal dispatching method of smart distribution network considering integrated energy microgrid with multiple gird-connected points," *IET Energy Systems Integration*, doi: 10.1049/esi2.12089

[38] J. Gholami, K. K. A. Ghany, and H. M. Zawbaa. "A novel global harmony search algorithm for solving numerical optimizations," *Soft Computing*, vol. 25, pp. 2837-2849, Feb. 2021.

[39] A. Kumar and G. Shankar. "Dynamic stability enhancement of TCSC-based tidal power generation using quasi-oppositional harmony search algorithm," *IET Generation, Transmission & Distribution*, vol. 12, no. 10, pp. 2288-2298, Mar. 2018.

Bing Sun received the B.E. degree in electrical engineering from Tianjin University, Tianjin, China, in 2011, and the Ph.D. degree in electrical engineering from Tianjin University, in 2017. He is currently an Associate Professor and Master Tutor in the School of Electrical and Information Engineering at Tianjin University. His main research interests include distributed optimal operation of smart distribution network and renewable energy planning and consumption effect improvement method.

Ruipeng Jing received the B.E. degree in electrical engineering from Hebei University of Technology, Tianjin, China, in 2021. He is currently pursuing the Master degree in the School of Electrical and Information Engineering at Tianjin University, Tianjin, China. His main research interests include distributed operation of smart distribution network and distributed resource planning.

Leijiao Ge received the B.E. degree in electrical engineering from Beihua University, Jilin, China, in 2006, the master degree in electrical engineering from Hebei University of Technology, Tianjin, China, in 2009, and the Ph.D. degree in electrical engineering from Tianjin University, Tianjin, China, in 2016. He is currently an Associate Professor in the School of Electrical and Information Engineering at Tianjin University. His main research interests include smart distribution network, cloud computing and big data.

Yuan Zeng received the B.E. degree in electrical engineering from Tianjin University, Tianjin, China, in 2002, and the Ph.D. degree in electrical engineering from Tianjin University, in 2007. He is currently an Associate Professor in the School of Electrical and Information Engineering at Tianjin University. His main research interests include operation and planning of smart distribution network.

Shimeng Dong received the B.E. degree in electrical engineering from Tianjin University, Tianjin, China, and the master degree in Department of Electrical Engineering, Tsinghua University, Beijing, China. He is currently an Engineer in State Gird Corporation of China, Beijing, China. His main research interests include operation and planning of smart distribution network.

Luyang Hou received the Ph.D. degree in information systems engineering from Concordia University, Montreal, Canada, in 2020. He is currently a Lecturer in the School of Computer Science (National Pilot Software Engineering School), Beijing University of Posts and Telecommunications, Beijing, China. His main research interests include energy internet, vehicle edge computing, and artificial intelligence.